Hindawi Publishing Corporation
Physics Research International
Volume 2011, Article ID 583420, 10 pages
doi:10.1155/2011/583420

Research Article

Electrical Conductivity and Dielectric Properties of Bulk Glass V_2O_5 (ZnO, PbO) SrO FeO

M. S. Aziz,[1] A. G. Mostafa,[2] A. M. Youssef,[1] and S. M. S. Youssif[1]

[1] *Physics Department, Faculty of Science in Damietta, Mansoura University, Damietta, Egypt*
[2] *ME Laboratory, Physics Department, Faculty of Science, Al-Azhar University, Nasr City, Cairo, Egypt*

Correspondence should be addressed to S. M. S. Youssif, smsmy75@hotmail.com

Received 29 October 2010; Accepted 22 February 2011

Academic Editor: Anil Chourasia

The AC conductivity and dielectric parameters of the glassy system of (70-x) $V_2O_5 \cdot x$(Zn/Pb)·10SrO·20FeO (x = 0, 5, 10, and 15) glasses have been investigated. The frequency and temperature dependence of dielectric constant (ε') and dielectric loss (ε'') is studied in the frequency range 100 Hz–5 MHz and in the temperature range 300–460 K. Dielectric dispersion is observed in all samples as Zn/Pb increase content in the (70-x)$V_2O_5 \cdot x$ (Zn/Pb)·10SrO·20FeO systems. These results are explained on the basis of a Debye-type relaxation. It is also observed that the activation energy increases on increasing the Zn/Pb contents in this system.

1. Introduction

Transition metal (TM) oxide glasses have been of great interest and have drawn much attention in recent years due to their possible technological applications in memory switching, electrical threshold, optical switching devices, and so forth [1–3]. These glasses show semiconducting properties that arise from the presence of more than one valence state of the TM ions [4, 5].

Although the transition metal ion glasses based on conventional network formers, such as P_2O_5, GeO_2, and SiO_2 have been studied extensively [5, 6], there are a few reports on the glasses containing transition metal oxides as glass network formers [7–9]. Further, although the existence of binary V_2O_5 glasses is well established, their structure has been studied relatively little and as a result there is no clear picture as to the exact nature of the oxygen polyhedral surrounding the vanadium atoms or of the role played by the second component. Even in the case of pure V_2O_5 glass it has been reported in the literature [10] that V^{5+} ions exhibit both 4- and 5-fold coordination states, which is related to the sample preparation conditions.

A critical analysis of this problem has been published by Wright [11]. It has been observed [7–9] that the structure of these vanadate glasses depends on the nature of the network formers as well as on the network modifiers.

These types of glasses exhibit mixed electronic (electrons hopping along V^{4+}-O-V^{5+} paths) and ionic (Sr^{2+} ions) conductivity. Glasses with such mixed electrical conductivity attract scientific interest because of potential applications as solid electrolytes in electrochemical devices such as batteries, chemical sensors, and smart windows.

2. Sample Preparation and Experimental Techniques

The unconventional TMO glasses were prepared by the conventional melt quenching method on the basis of molecular formula [(70-x)$V_2O_5 \cdot xR$·10SrO · 20FeO, where R = ZnO, PbO and, $0 \le x \le 15$]. Chemically pure materials were used to prepare the glass batches. The finely mixed batches were melted in porcelain crucibles in an electrically heated muffle furnace at temperatures ranging between 850 and 950°C depending on the composition of the batches. The duration of melting was 2 hours, and the melts were swirled several times to ensure complete homogeneity as well as to obtain bubble free melts. The solid glass samples were obtained by pressing the melt between two precooled stainless steel plates.

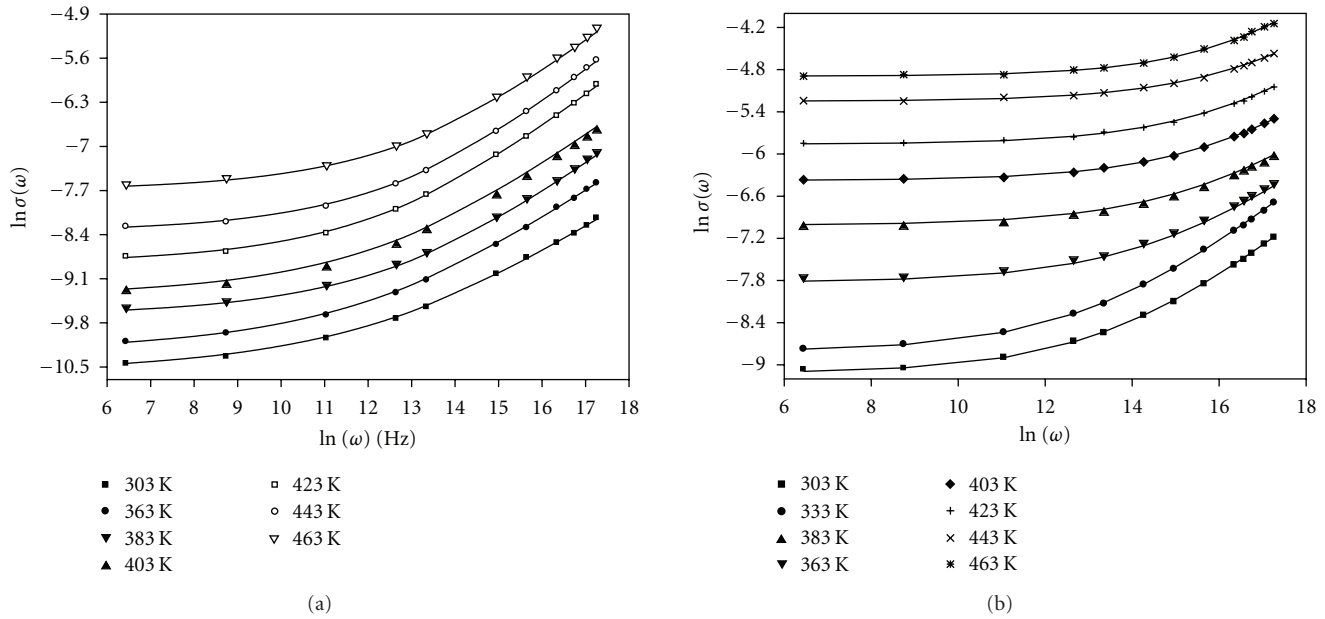

Figure 1: Frequency dependence of AC conductivity (σ_{ac}) at various temperatures for the samples (a) x = 10% mole ZnO glass and (b) x = 10% mole PbO glass.

The produced samples were annealed at 200°C overnight with decreasing temperature rate of about 1°C\3.5 mints, in order to remove stress and strain.

For electrical measurements, the annealed samples were polished to obtain disk shape samples with 2 mm thickness and 7 mm diameter. Good electrical content was achieved by painting the faces of the samples with an air-dried silver paste. The temperature of the sample was measured using digital thermometer.

The AC conductivity $\sigma(\omega)$, dielectric constant (ε'), and dielectric loss (ε'') were carried out on a Hioki 3532 LCR Hitester from 100 Hz to 5 MHz in the temperature range 297–473 K. This LCR bridge measures the frequency (f), capacitance (C), impedance (Z), phase angle (Φ), and dissipation factor (tanδ). The dielectric constant (ε') and dielectric loss (ε'') can be calculated by applying the following relations [12]:

$$\varepsilon' = \frac{Cd}{(\varepsilon_o A)}, \tag{1}$$

$$\varepsilon'' = \frac{\sigma}{(\omega \varepsilon_o)}, \tag{2}$$

where d is the sample thickness, A the cross-sectional area, σ the conductivity, and ε_o the permittivity of free space (= 8.854×10^{-12} F/m).

3. Results and Discussions

The experimental results of the AC conductivity of (70-x)V_2O_5 ·x(ZnO, PbO) ·10SrO·20FeO glass system is taken in temperature range 300 K–473 K, in the frequency range of 100 Hz–5 MHz of the selected samples (x = 0, 5, 10, and 15). Figure 1 shows, as an example, the variation of the AC conductivity, σ_{ac}, as a function of frequency at several temperatures, for composition x = 10% mol ZnO and PbO, respectively. It was observed that a good fitting is with $\sigma_{ac}(\omega) = \sigma(0) + A\omega^s$ [13–15]. These results agree with all samples; there are very well fitted to AC conductivity functions (results not shown here). The frequency exponent s was computed from the slope of the straight lines. This shows that the value of s is temperature dependent in the investigated range of temperatures, and it was found that at x = 0 and 5% mole of ZnO it increases with temperature up to the maximum value $s \approx 0.36$, shown in Figure 2(a). But in the other samples (x = 10 and 15% mole) the frequency exponent s decreases with temperature decrease. This agrees with the studded samples of Pb glass system. In the PbO glass system it was found that also the frequency exponent s decrease with temperature increase, as well as the maximum value of s at low temperature $s \approx 0.6$ at x = 15%mole, and decreases to the low value $s \approx 0.06$, shown in Figures 3(a), 3(b), and 3(c). The above results indicates that the value of s is temperature dependent in the investigated range of temperatures. It can be seen here that, when ZnO/PbO concentration increases, there is a corresponding decrease in the vanadium. From these it was said that ZnO/PbO maybe begins to behave like a network former. From AC models this results nearly agree with the CBH model for samples 15% mol in PbO glass system and 10% and 15% mole of ZnO. But at 0% and 5% mole ZnO agree with small polaron tunnelling (SP), and finally at 5% and 10% mole PbO the results agree with the overlapping-polaron model (OLP).

In most amorphous materials a polaron is formed due to the lattice distribution [16], and if small polarons are formed, the tunneling model predicts a decrease in s with decrease in

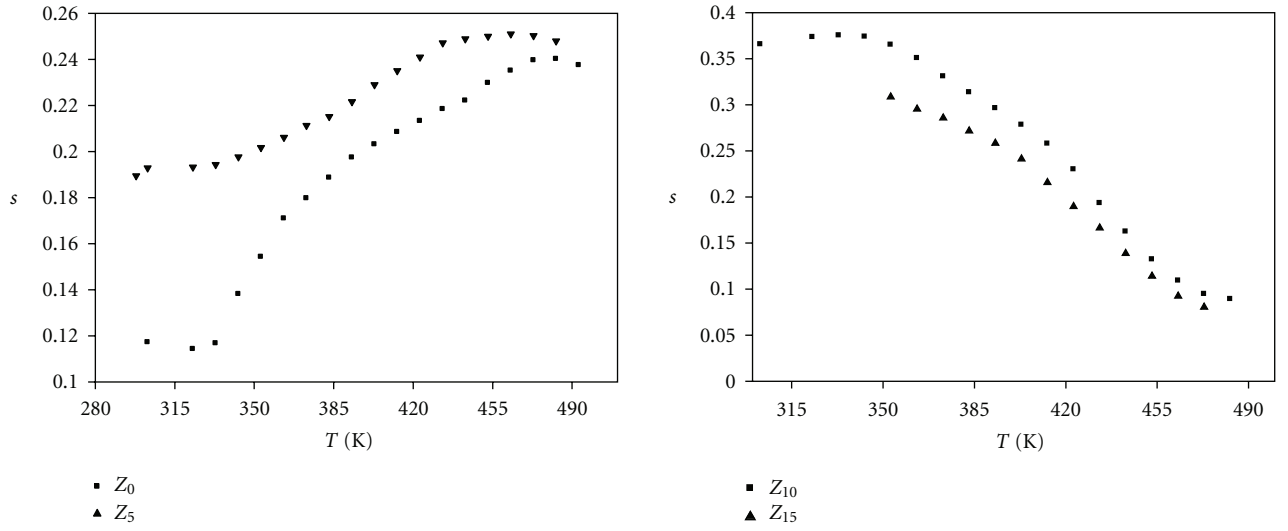

Figure 2: Frequency exponent s as a function of temperature for ZnO glass system (a) $x = 0$ and 5, (b) $x = 10$ and 15 at frequencies 120 Hz–5 MHz.

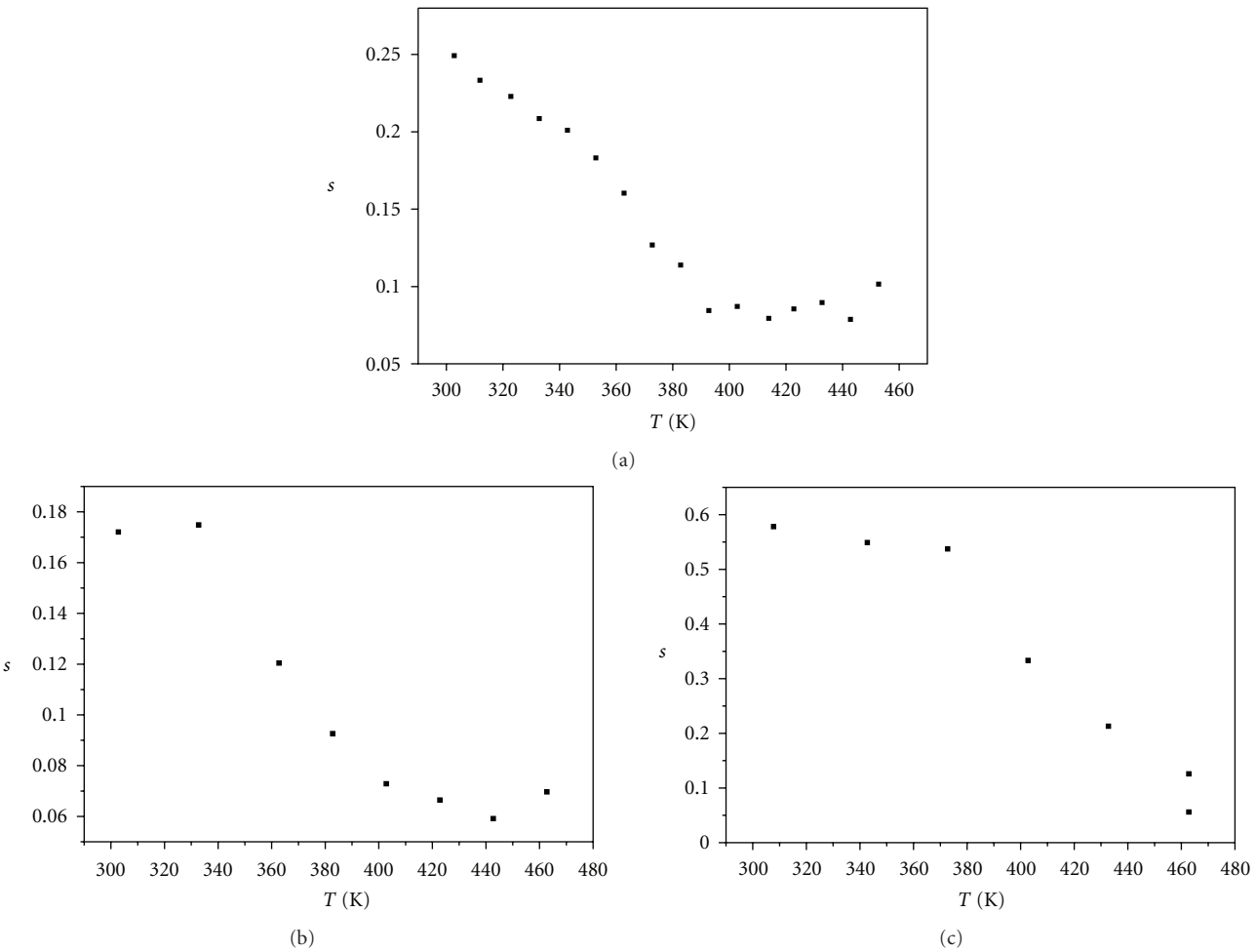

Figure 3: Frequency exponent s as a function of temperature for PbO glass system (a) $x = 5$, (b) $x = 10$, (c) $x = 15\%$ mole at frequencies (100 Hz–5 MHz).

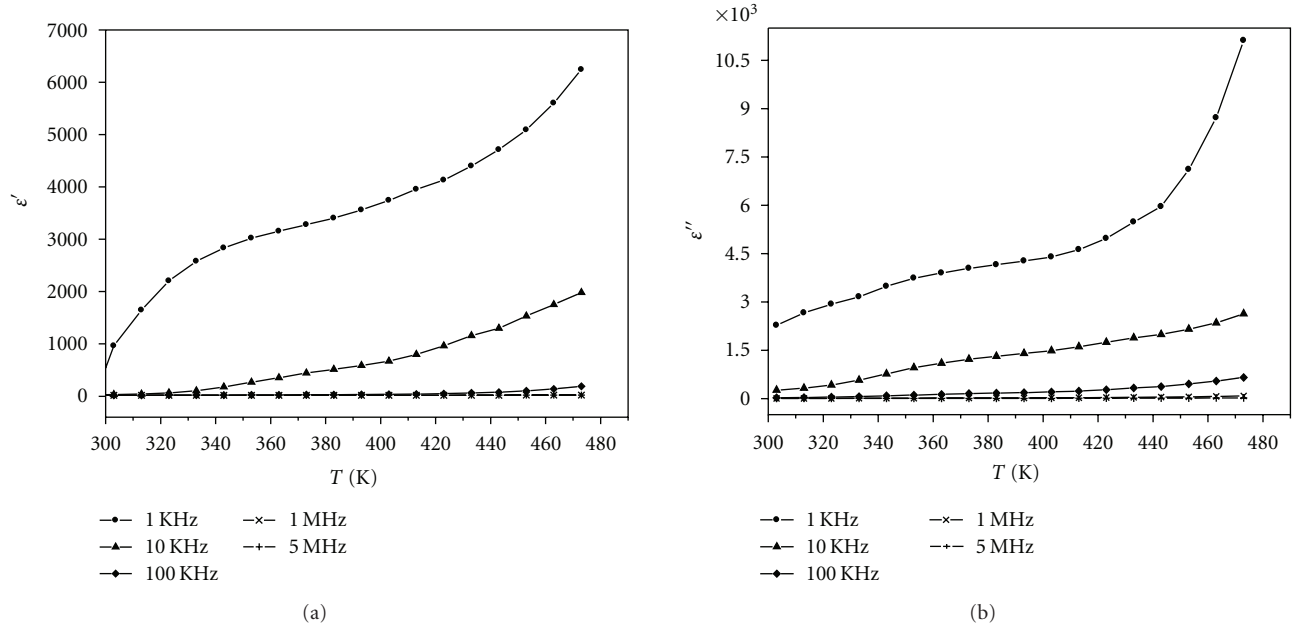

Figure 4: Typical plots of variation of (a) dielectric constant (ε') and (b) dielectric loss (ε'') parts of the dielectric constant with temperature for sample x = 0% mole ZnO at different frequencies.

temperature (Figure 2(a)). On the other hand, if overlapping large polarons are formed, the tunneling model predicts a decrease in s with increase in temperature up to a certain range and then an increase in s with a further increase in temperature (Figures 3(a) and 3(b)).

Hopping between two energetically favorable sites over a potential barrier may take place in TM oxide glasses. In the CBH model for AC loss, first introduced by Anderson and Drago [17] for single-electron hopping and extended by Elliott [18] for two-electron hopping simultaneously, the charge carrier is assumed to hop between site pairs over the potential barrier separating them. For neighboring sites at a separation R, the coulomb wells overlap, resulting in lowering of the effective barrier height from W_M to a value W which is given by equation [18]

$$\left(W = W_M - \left(\frac{e^2}{\pi\varepsilon\varepsilon_o R}\right)\right), \tag{3}$$

where W_M is the energy required completely to remove the electron from the site (into extended states) with $n = 1$ for single-electron hopping and $n = 2$ for two-electron CBH model. The frequency exponent s for this model is temperature dependent; s decreases from unity with increasing temperature from the experimental data, shown in Figure 2(b).

4. Dielectric Properties

The temperature dependence of the dielectric constant (ε') and the dielectric loss (ε'') is studied at various frequencies (100 Hz–5 MHz) for the selected glassy samples (70-x)$V_2O_5 \cdot x$(ZnO/PbO) $\cdot$ 10SrO $\cdot$ 20FeO (x = 0, 5, 10, and 15). The temperature range of measurement was from 300 to 460 K.

The dielectric constant ε' (real part) and dielectric loss ε'' (imaginary parts) of the complex dielectric constant were calculated from the relations (1) and (2). The data were also analyzed using the electrical modulus formalism [12]. The real (M') and imaginary (M'') parts of the complex electrical modulus ($M^* = 1/\varepsilon^*$) were obtained from ε' and ε'' values using the relations [12]

$$M' = \frac{\varepsilon'}{(\varepsilon'^2 + \varepsilon''^2)}, \qquad M'' = \frac{\varepsilon''}{(\varepsilon'^2 + \varepsilon''^2)}. \tag{4}$$

5. Temperature and Frequency Dependence of the Dielectric Constant $\varepsilon'(\omega)$ and Dielectric Loss $\varepsilon''(\omega)$ of Samples

The variation of real (ε') and imaginary (ε'') parts of dielectric constant with temperature for sample Z_0 (x = 0% mole) at different frequencies is shown in Figure 4. It was shown in all studied sample (70-x) $V_2O_5 \cdot x$(ZnO/PbO) $\cdot$ 10SrO $\cdot$ 20FeO (x = 0, 5, 10, and 15) systems that

(1) the dielectric constant (ε') and the dielectric loss (ε'') increase with the increasing temperature in a different way for different frequencies,

(2) dielectric dispersion is observed clearly from 300 K,

(3) the variation of the dielectric constant (ε') and the dielectric loss (ε'') with temperature is larger at lower frequencies.

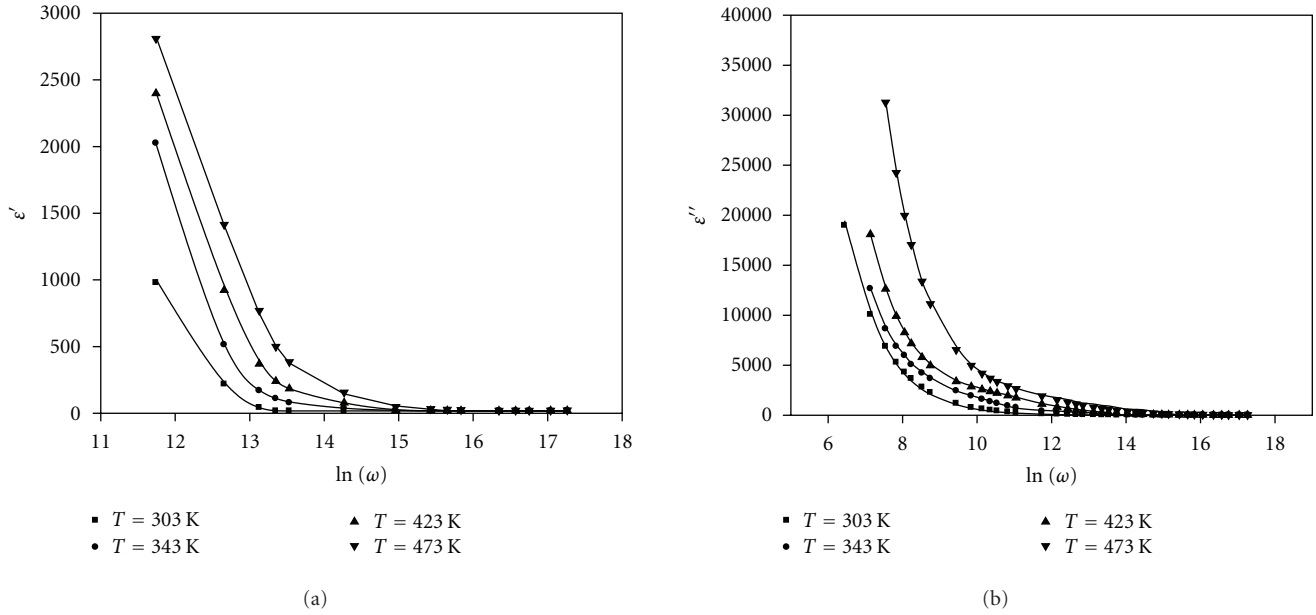

Figure 5: Typical plots of variation of (a) dielectric constant (ε') and (b) dielectric loss (ε'') parts of the dielectric constant with frequency for sample x = 0% mole ZnO at different temperatures.

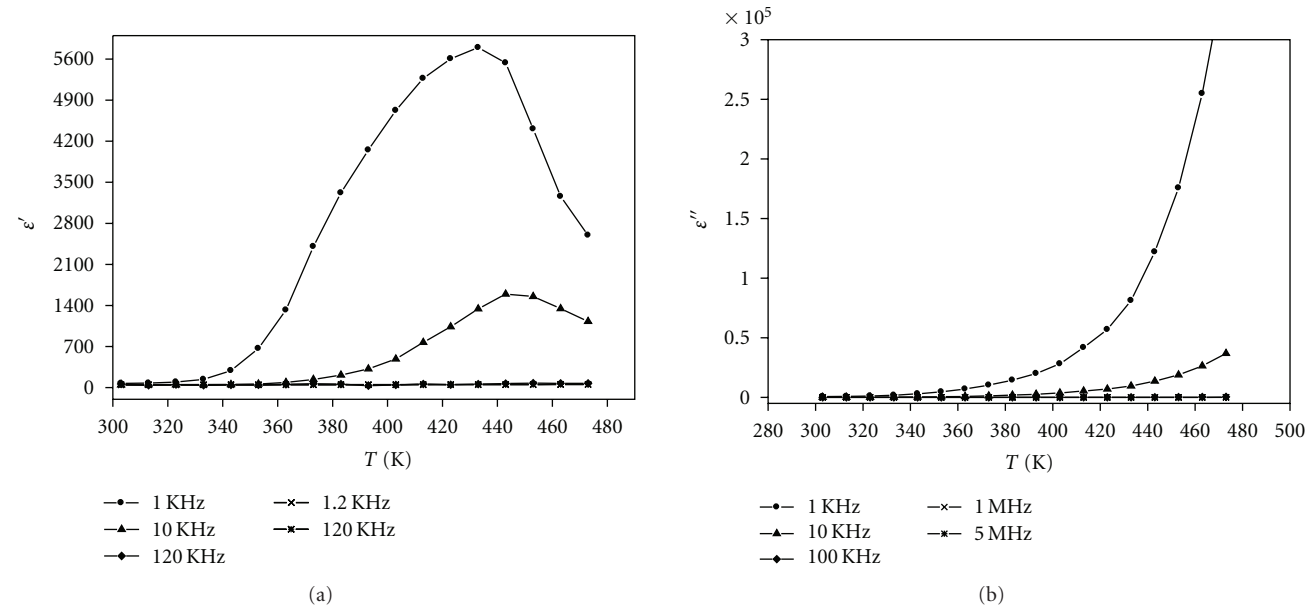

Figure 6: Typical plots of variation of (a) dielectric constant (ε') and (b) dielectric loss (ε'') parts of the dielectric constant with temperature for sample x = 10%mole ZnO at different frequencies.

These results agree with all the studied samples (70-x) $V_2O_5 \cdot x$(ZnO/PbO) · 10SrO · 20FeO (x = 5, 10, and 15% mole).

Figure 5 shows the frequency response of the dielectric constant and the dielectric loss (ε'') at different fixed temperatures for the Z_0 (x = 0) sample. It is observed that the dielectric constant (ε') and the dielectric loss decrease on increasing the frequency. These results agree with all the studied samples (70-x) $V_2O_5 \cdot x$(ZnO/PbO) · 10SrO · 20FeO (x = 5, 10, and 15).

Figures 6 and 7 show the variation of the dielectric constant (ε') and the dielectric loss (ε'') with temperature at different frequencies for selected samples $(Zn/Pb)_x$, where x = 10. It was observed that, in both of two samples $(Zn/Pb)_x$, x = 10, the dielectric constant (ε') varies exponentially with temperature and that a strong dielectric dispersion

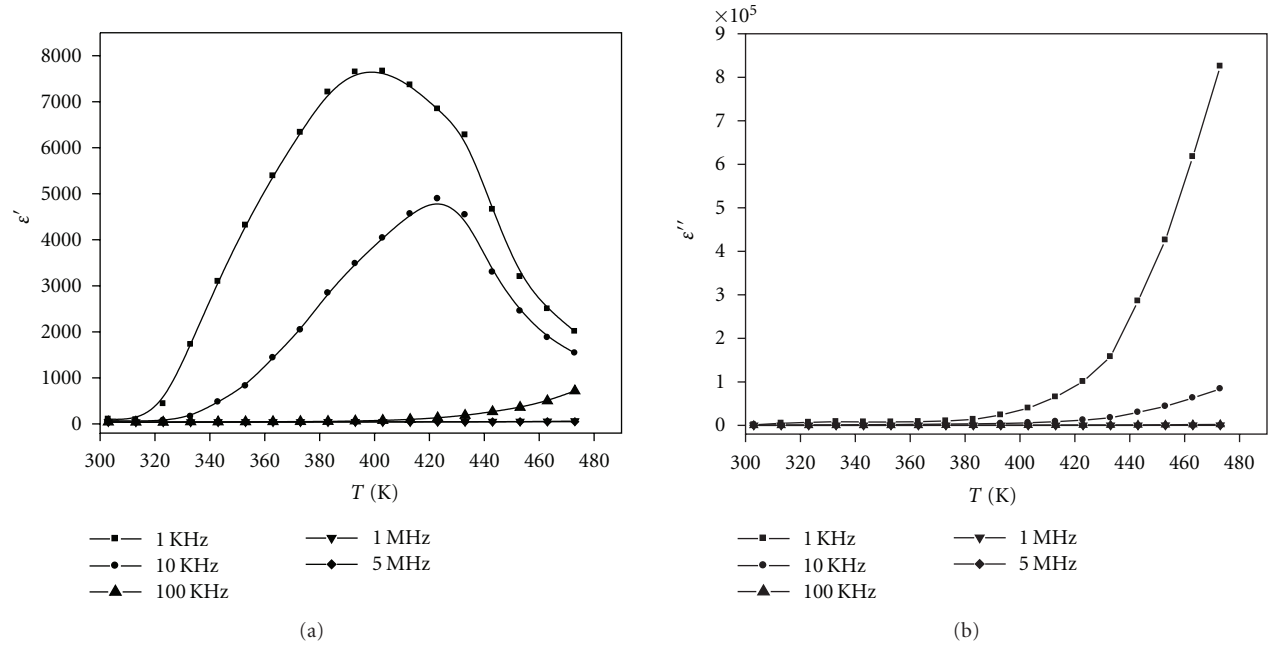

FIGURE 7: Typical plots of variation of (a) dielectric constant (ε') and (b) dielectric loss (ε'') parts of the dielectric constant with temperature for sample $x = 10\%$mole PbO at different frequencies.

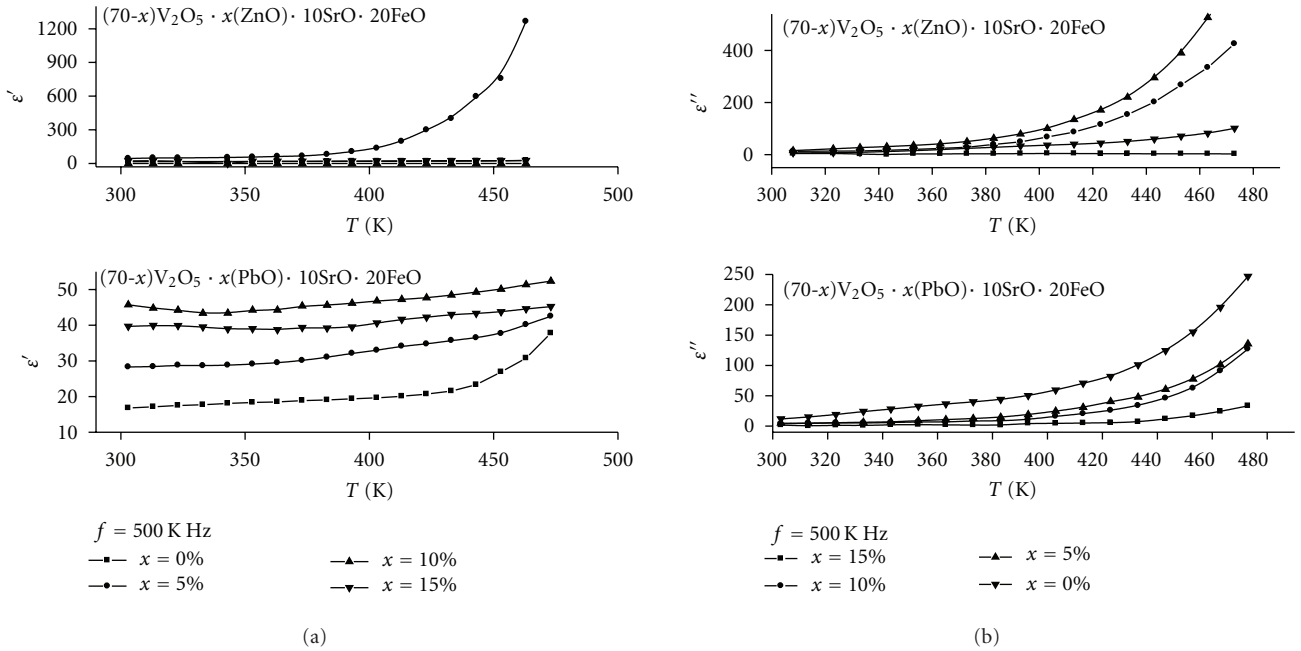

FIGURE 8: Variation of (a) dielectric constant and (b) dielectric loss with temperature at 5×10^5 Hz frequency for the (70-x)$V_2O_5 \cdot x$(ZnO) $\cdot$10SrO $\cdot$ 20FeO systems.

is observed at above 300 K and 340 K for Z_{10} and P_{10}, respectively. Also it was observed peaks in the ε'-T curves for different fixed frequencies; these peaks are shifted towards higher temperature as the frequency increases.

In the studied samples (70-x) $V_2O_5 \cdot x$(ZnO/PbO) $\cdot$ 10SrO $\cdot$ 20FeO (x = 5 and 15) (results not reported here) the dielectric constant (ε') increase with temperature is more clear at lower frequencies. The increase in the dielectric constant (ε') of the sample is due to the electric field which is accompanied by the applied frequencies; such field will cause some ordering inside the sample as well as the formation of an electric moment in the entire volume of the dielectric and in each separate polarizing molecule. The molecular dipoles in polar material cannot orient themselves

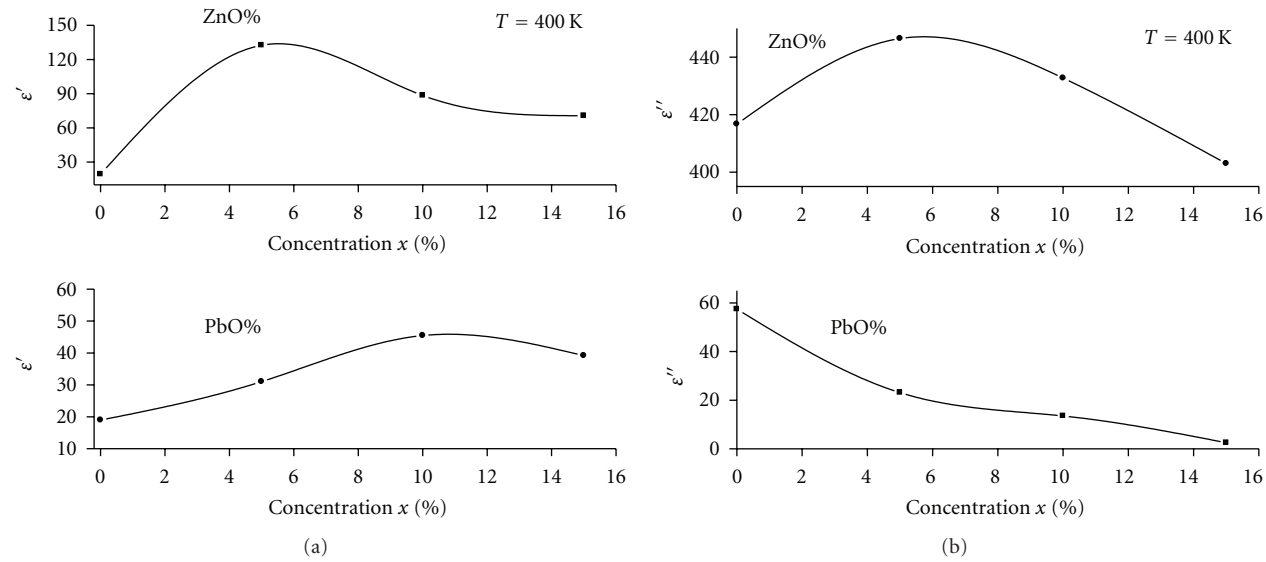

Figure 9: Variation of (a) dielectric constant and (b) dielectric loss with concentration for the (70-x)$V_2O_5 \cdot x$ (ZnO) $\cdot$ 10SrO $\cdot$ 20FeO systems.

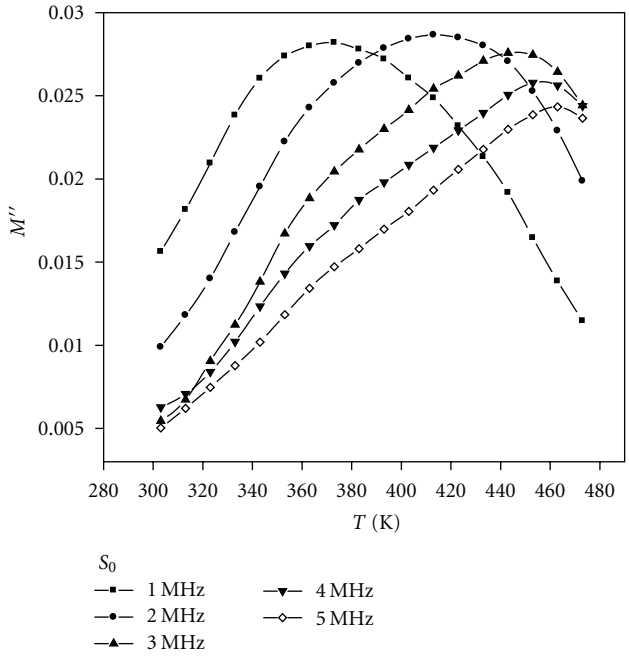

Figure 10: Typical plots of variation of imaginary (M'') part of the dielectric modulus with temperature for sample x = 10% mole ZnO at different frequencies.

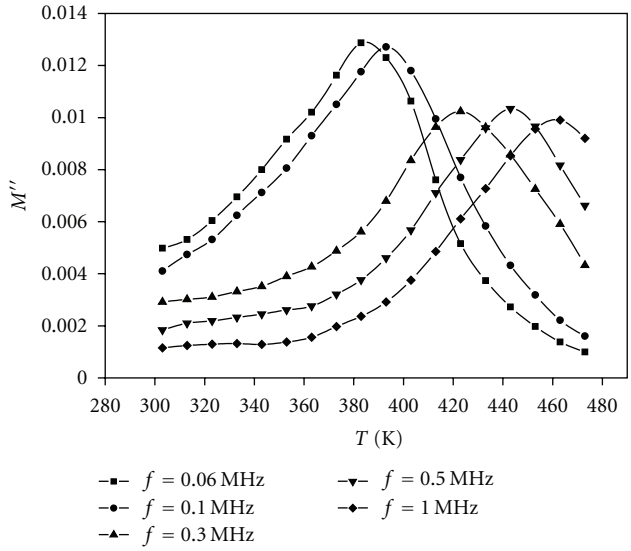

Figure 11: Typical plots of variation of imaginary (M'') part of the dielectric modulus with temperature for sample x = 10% mole ZnO at different frequencies.

at low temperature. When the temperature rises, the dipoles orientation is facilitated, and this increases the dielectric constant. In slowly varying fields at low frequency, the dipoles align themselves along the field direction and fully contribute to the total polarization. As the frequency is increased, the variation in the field becomes too rapid for the molecular dipoles to follow, so that their contribution to the polarization becomes less with a measurable lag because of internal frictional forces [19].

Figures 6 and 7 show the variation in the dielectric loss (ε'') as a function of temperature and frequency. These figures illustrate that the dielectric loss (ε'') exhibits strong temperature dependence at higher temperature and lower frequencies. Also the values of dielectric loss (ε'') increase with temperature as compared to a pure sample Z_0. These results agree with all samples (70-x) $V_2O_5 \cdot x$(ZnO/PbO) $\cdot$ 10SrO $\cdot$ 20FeO (x = 5 and 15) (results not shown here). These results indicate that the

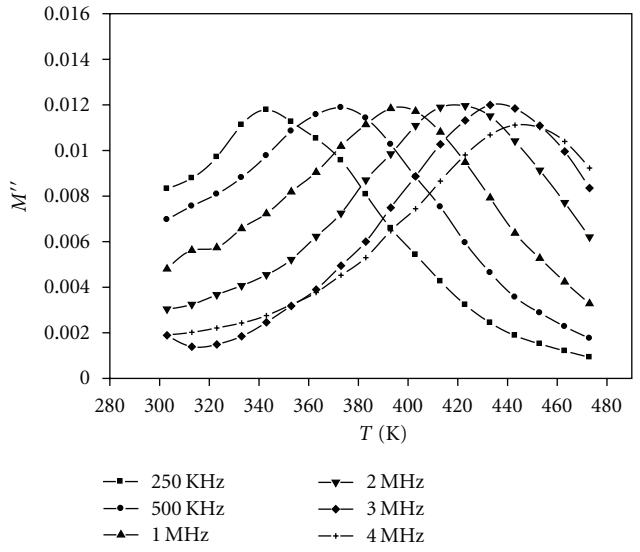

Figure 12: Typical plots of variation of imaginary (M'') part of the dielectric modulus with temperatures for sample $x = 10\%$ mole PbO at different frequencies.

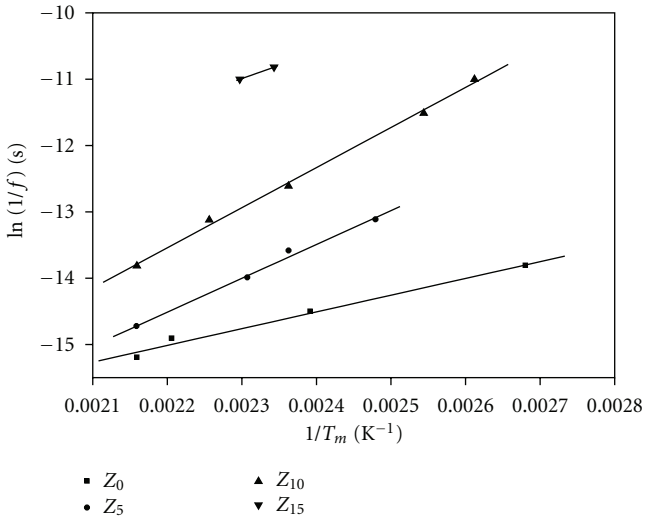

Figure 13: The variation of relaxation frequency with $1/T_m$.

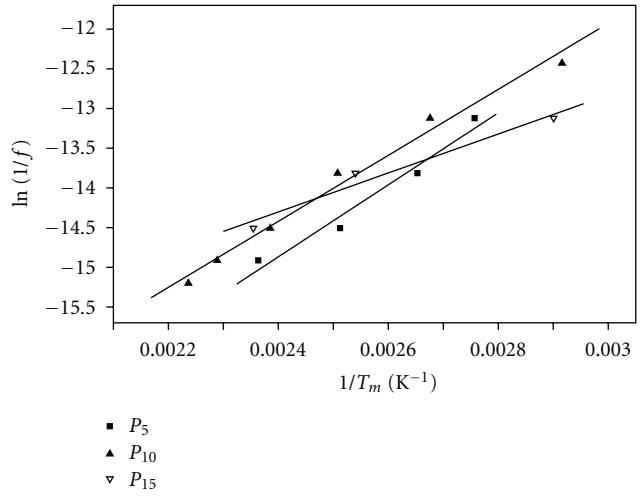

Figure 14: The variation of relaxation frequency with $1/T_m$.

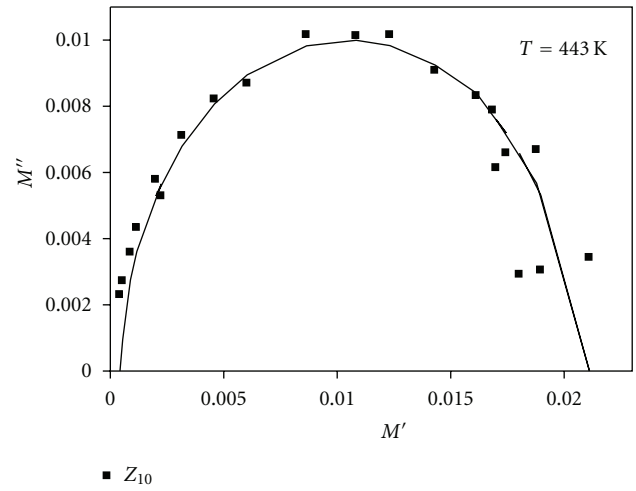

Figure 15: Cole-Cole diagram for the Z_x, $x = 10\%$ sample.

concentration of Zn and Pb plays an important role in the variation of dielectric parameters with temperature. Owing to Stevels [20], the origins of the dielectric loss (ε'') are conduction losses, dipole losses, and vibration losses. As the temperature increases, the electrical conduction losses increase, which increases the dielectric loss (ε'').

Figures 8(a) and 8(b) show the variation of the dielectric constant (ε') and the dielectric loss (ε'') with temperature for different concentrations of zinc and lead at a fixed frequency (5×10^5 Hz). It is clear from these figures that the dielectric constant (ε') and the dielectric loss (ε'') both increase with zinc and lead concentration in (70-x) $V_2O_5 \cdot x$(ZnO/PbO) $\cdot$ 10SrO $\cdot$ 20FeO (x = 0, 10, 5, and 15) systems.

Figures 9(a) and 9(b) show the variation of the dielectric constant (ε') and the dielectric loss (ε'') with zinc/lead concentration at fixed temperature ($T = 400$ K).

Mott et al. [21] and Kastner et al. [22] have proposed an interesting model for chalcogenide glasses. They suggest that the states in the gap, near Fermi level, are due to dangling bonds, and, if the reaction $2D_o \rightarrow D_+ + D_-$ is exothermic, then only paired, defect states are found in the gap. Since these defect states are paired in which half of the charge carriers (dangling bonds) are positively charged and the remaining half are negatively charged, the paired states analogous to electric dipoles and hence the entire system may be considered to be virtually a dipolar system. At low temperature, one would expect a large distribution of relaxation times because of hindered rotation of these dipoles. Therefore, a Debay-type relaxation may lose its significance at such low temperatures. A very large distribution of relaxation times should give a dielectric loss which would be almost independent of temperature. As the

Table 1: Dielectric relaxation parameters of $(70\text{-}x)V_2O_5 \cdot x(ZnO/PbO) \cdot 10SrO \cdot 20FeO$, ($x = 0, 5, 10, 15$).

Samples	T(K)	ε_∞	ε_s	τ	τ_0	Relaxation time from Cole-Cole τ	α	ΔE_{dc}	ΔE_{ac}
Z_0	343 K	45	4100	2.4×10^{-5}	1.16×10^{-9}	3.5×10^{-4}	0.61	0.41	0.35
Z_5	383 K	35	8300	2.7×10^{-4}	6.67×10^{-12}	4.5×10^{-3}	0.5	0.43	0.43
Z_{10}	383 K	36	18700	3.3×10^{-4}	2.2×10^{-12}	3×10^{-5}	0.51	0.53	0.52
Z_{15}	433 K	40	21100	2.5×10^{-4}	1.84×10^{-9}	3×10^{-4}	0.59	0.70	0.69
P_5	373 K	42	150	5.4×10^{-6}	6.55×10^{-12}	5.2×10^{-2}	0.5	0.53	0.48
P_{10}	403 K	46	140	3.5×10^{-6}	3.58×10^{-11}	1.35×10^{-4}	0.31	0.65	0.53
P_{15}	383 K	20	100	1.4×10^{-3}	1.69×10^{-9}	3.1×10^{-4}	0.60	0.65	0.56

temperature increases, the dipoles slowly attain freedom of rotation, and, therefore, a Debye-type relaxation should be observable. Under such circumstances, the dielectric loss is expected to become temperature and frequency dependent.

According to Debye's theory [23, 24] of intrinsic relaxation time, the experimental data of (ε') and (ε'') become fit by equations:

$$\varepsilon'(\omega) = \varepsilon_\infty + \frac{(\varepsilon_s - \varepsilon_\infty)}{(1 + \omega^2\tau^2)},$$
$$\varepsilon''(\omega) = \frac{(\varepsilon_s - \varepsilon_\infty)\omega\tau}{(1 + \omega^2\tau^2)}, \quad (5)$$

where ε_s and ε_∞ are the static and optical dielectric constants and τ is the relaxation time. All the studied samples $(70\text{-}x)V_2O_5 \cdot x(Zn/Pb) \cdot 10SrO \cdot 20FeO$, $x = 0$, 5, 10 and 15% mole well agree with the fitting with Debye's theory. The values of ε_s, ε_∞, and τ given in Table 1.

6. Dielectric Modulus

The AC response of the investigated samples $(70\text{-}x)V_2O_5 \cdot x(ZnO/PbO) \cdot 10SrO \cdot 20FeO$ ($x = 0$, 5, 10, 15) has been examined by the variation of real (M') and imaginary (M'') parts of the dielectric modulus. The real (M') and imaginary (M'') part of the dielectric modulus as a function of frequency for glass samples shown in Figures 11, 12, and 13 as example. At all the samples it was shown that there are peaks in the M''-T curves that shift to higher temperatures for higher frequencies. This reveals that, when the frequency is high, the temperature at which measuring frequency is equal to f_c is also high.

The peak positions of M'' give the temperature at which the measuring frequency is equal to the conductivity relaxation frequency f_c which is given by the relation [25]

$$f_c = \nu_c \exp\left(-\frac{W_c}{k} T_m\right), \quad (6)$$

where ν_c is the characteristic phonon frequency and W_c the activation energy for conductivity relaxation. Values of characteristic relation time $\tau_o(\nu_c = 1/\tau_o)$ have been evaluated from the plots of $\ln(1/f_c)$ $\nu_s \cdot 1/T_m$, where T_m is the temperature at the peak for certain frequency, shown in Figures 14 and 15, the values of τ_o are given in Table 1.

Cole and Cole showed that, if a dielectric system has a distribution of relaxation time, the curve obtained by plotting M'' versus M' is generally an arc of a circle interesting the abscissa axis at the values of ε_∞ and ε_s. Shows Figure 15 Cole-Cole diagram, for example, to Zn_x, $x = 10$, all samples $(70\text{-}x)V_2O_5 \cdot x(ZnO/PbO) \cdot 10SrO \cdot 20FeO$ ($x = 0$, 5, and 15) show this regime.

The dielectric constant and loss data of the samples ($x = 0$, 5, 10, and 15% mole ZnO/PbO) were fitted to the Cole-Cole function [26] at $T = 473$ K:

$$\varepsilon' = \varepsilon_\infty + \left(\frac{[(\varepsilon_o - \varepsilon_\infty)\ (1 + (\omega\tau)(1-\alpha)\,\mathrm{Sin}(\alpha\pi/2)\,]}{[1 + 2(\omega\tau)(1-\alpha)\,\mathrm{Sin}(\alpha\pi/2) + (\omega\tau)2(1-\alpha)]}\right),$$
$$\varepsilon' = \varepsilon_{dc} + \left(\frac{[(\varepsilon_o - \varepsilon_\infty)\ ((\omega\tau)(1-\alpha)\,\mathrm{Cos}(\alpha\pi/2)\,]}{[1 + 2(\omega\tau)(1-\alpha)\,\mathrm{Sin}(\alpha\pi/2) + (\omega\tau)2(1-\alpha)]}\right), \quad (7)$$

where α is the Cole-Cole distribution parameter having values between 0 and 1. The parameters τ and α are given in Table 1. The agreement between theoretical and experimental values is very good in the high-frequency tail regime at all temperatures measured.

7. Conclusion

The dielectric parameters and the electrical properties of the studied glass systems were found to be temperature and frequency dependent. A dielectric dispersion was found to occur in these two systems. Such dispersion was supposed to be due to the dc conduction loss as well as to the dipolar type of the defects in the studied samples. The dielectric constant and the dielectric loss show slight increase with the addition of ZnO until it reached a maximum value in the sample containing 10 mol% but on adding PbO to the vanadate network, they show a decrease to reach its smallest value at 15 mol% PbO. A possible explanation for glasses containing ZnO is given in terms of hopping of charge carriers over a potential barrier between charged defect states. The increase of the dielectric parameters with zinc oxide concentration can be understood in terms of the decreased density of defect states. In glasses containing PbO, it can be stated that the density of defect states increased when lead oxide concentration was increased.

On increasing the concentrations of zinc or lead oxides, an increase in the activation energies was observed, which

may be due to the decrease of the density of defect states and/or to the decrease of the disorder in the mobility edge. Complex relative permittivity data have been analyzed using the dielectric modulus (M' and M'') approach where a single relaxation process was observed. The values of the activation energy for conductivity relaxation were found to be less than those evaluated from dc conductivity for all the studied glasses.

The dielectric constant and loss data of all glasses were fitted to Cole-Cole functions, where the parameter α was found to be zero, while the relaxation time τ varies between $5.2 \times 10{-}2$ and $3 \times 10{-}2$ s.

References

[1] A. Ghosh, "Memory switching in bismuth-vanadate glasses," *Journal of Applied Physics*, vol. 64, no. 5, pp. 2652–2655, 1988.

[2] J. Livage, J. P. Jolivet, and E. Tronc, "Electronic properties of mixed valence oxide gels," *Journal of Non-Crystalline Solids*, vol. 121, no. 1–3, pp. 35–39, 1990.

[3] Y. Sakurai and J. Yamaki, "V//2O//5-P//2O//5 GLASSES AS CATHODE FOR LITHIUM SECONDARY BATTERY," *Journal of the Electrochemical Society*, vol. 132, no. 2, pp. 512–513, 1985.

[4] N. Mott, "Conduction in glasses containing transition metal ions," *Journal of Non-Crystalline Solids*, vol. 1, no. 1, pp. 1–17, 1968.

[5] G. D. Khattak, E. E. Khawaja, L. E. Wenger et al., "Composition-dependent loss of phosphorus in the formation of transition-metal phosphate glasses," *Journal of Non-Crystalline Solids*, vol. 194, no. 1-2, pp. 1–12, 1996.

[6] G. D. Khattak and N. Tabet, "Local structure and redox state of vanadium in strontium-vanadate glasses," *Journal of Electron Spectroscopy and Related Phenomena*, vol. 136, no. 3, pp. 257–264, 2004.

[7] Y. Dimitriev, V. Dimitrov, M. Arnaudov, and D. Topalov, "IR-spectral study of vanadate vitreous systems," *Journal of Non-Crystalline Solids*, vol. 57, no. 1, pp. 147–156, 1983.

[8] A. C. Wright, C. A. Yarker, P. A. V. Johnson, and R. N. Sinclair, "A neutron diffraction investigation of the structure of phosphorus, barium and lead vanadate glasses," *Journal of Non-Crystalline Solids*, vol. 76, no. 2-3, pp. 333–350, 1985.

[9] S. Hayakawa, T. Yoko, and S. Sakka, "Structural studies on alkaline earth vanadate glasses (part 2)—V NMR spectroscopic study -," *Journal of the Ceramic Society of Japan*, vol. 102, no. 6, pp. 530–535, 1994.

[10] M. Nabavi, C. Sanchez, and J. Livage, "Structure and properties of amorphous V_2O_5," *Philosophical Magazine*, vol. 63, no. 4, pp. 941–953, 1991.

[11] A. C. Wright, *Philosophical Magazine*, vol. 50, p. 23, 1984.

[12] M. H. Bhat, M. Kandavel, M. Ganguli, and K. J. Rao, "Li ion conductivities in boro-tellurite glasses," *Bulletin of Materials Science*, vol. 27, no. 2, pp. 189–198, 2004.

[13] D. P. Almond, A. R. West, and R. J. Grant, "Temperature dependence of the a.c. conductivity of Naβ-alumina," *Solid State Communications*, vol. 44, no. 8, pp. 1277–1280, 1982.

[14] D. P. Almond, G. K. Duncan, and A. R. West, "The determination of hopping rates and carrier concentrations in ionic conductors by a new analysis of ac conductivity," *Solid State Ionics*, vol. 8, no. 2, pp. 159–164, 1983.

[15] D. P. Almond, C. C. Hunter, and A. R. West, "The extraction of ionic conductivities and hopping rates from a.c. conductivity data," *Journal of Materials Science*, vol. 19, no. 10, pp. 3236–3248, 1984.

[16] N. F. Mott and E. A. Davis, *Electronic Properties in Non—Crystalline Materials*, Oxford Clarendon Press, Oxford, UK, 1979.

[17] S. E. Anderson and R. S. Drago, "The CBH model was introduced by Pike to account for the dielectric loss in scandium oxide," *Physical Review B*, vol. 6, p. 1527, 1972.

[18] S. R. Elliott, "Prediction of pulmonary function abnormalities after adult respiratory distress syndrome (ARDS)," *Advances in Physics*, vol. 36, p. 135, 1987.

[19] M. M. El-Nahass, A. F. El-Deeb, H. E. A. El-Sayed, and A. M. Hassanien, "Electrical conductivity and dielectric properties of bulk glass SeGeAs chalcogenide," *Physica B*, vol. 388, no. 1-2, pp. 26–33, 2007.

[20] J. M. Stevels, in *Handbuch der Physik*, S. Flugge, Ed., p. 350, Springer, Berlin, Germany, 1957.

[21] N. F. Mott, E. A. Davis, and R. A. Street, "States in the gap and recombination in amorphous semiconductors," *Philosophical Magazine*, vol. 32, no. 5, pp. 961–996, 1975.

[22] M. Kastner, D. Adler, and H. Fritzsche, "Valence-alternation model for localized gap states in lone-pair semiconductors," *Physical Review Letters*, vol. 37, no. 22, pp. 1504–1507, 1976.

[23] K. K. Srivastava, A. Kumar, O. S. Panwar, and K. N. Lakshminarayan, "Dielectric relaxation study of chalcogenide glasses," *Journal of Non-Crystalline Solids*, vol. 33, no. 2, pp. 205–224, 1979.

[24] D. Armitage, D. E. Brodie, and P. C. Eastman, "Switching in amorphous semiconductors," *Canadian Journal of Physics*, vol. 48, no. 22, pp. 2780–2782, 1970.

[25] H. El Mkami, B. Deroide, R. Backov, and J. V. Zanchetta, "Dc and ac Conductivities of (VO)(BO) oxide glasses," *Journal of Physics and Chemistry of Solids*, vol. 61, no. 5, pp. 819–826, 2000.

[26] K. S. Cole and R. H. Cole, "Dispersion and absorption in dielectrics," *Journal of Chemical Physics*, vol. 9, p. 341, 1941.